Chem

CellPress

Article

Integrating Superwettability within Covalent Organic Frameworks for Functional Coating

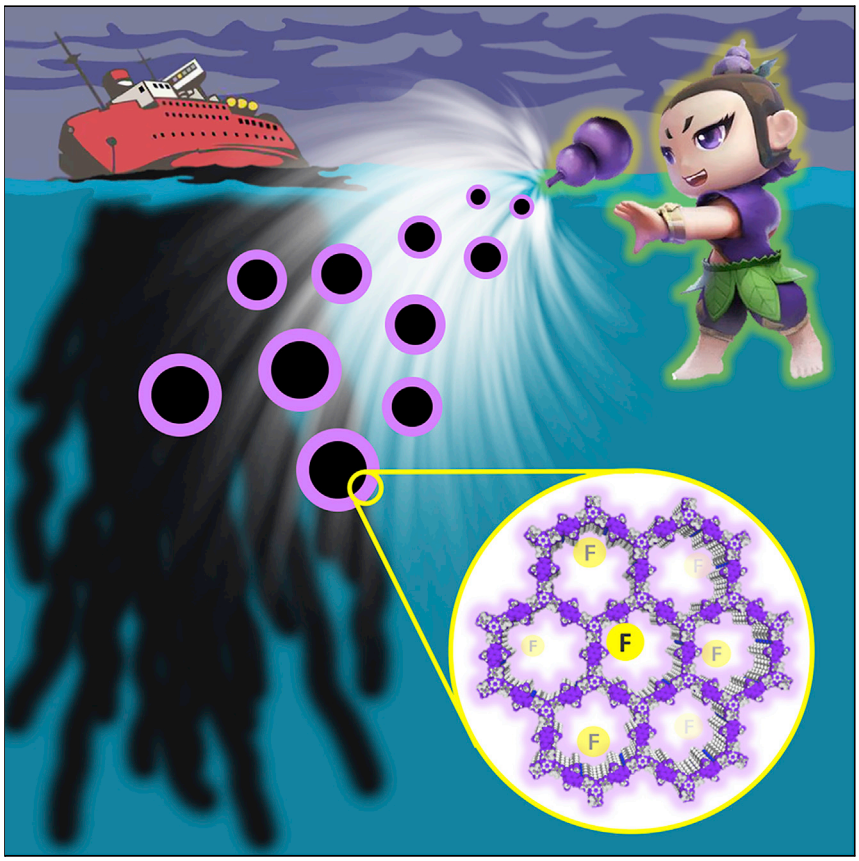

A COF material was imparted with superhydrophobicity via controllable pore-surface engineering while retaining porosity and crystallinity. Benefiting from the bulk superhydrophobicity of the COF and the feasibility of COF synthesis, it can be used as a coating or be *in situ* integrated within various devices; once applied, this renders them superhydrophobic. By combining the intrinsic properties of COFs and the bulky superhydrophobicity, such nanocoatings hold great potential in water remediation, device protection, and microfluidic applications.

Qi Sun, Briana Aguila, Jason A. Perman, Taylor Butts, Feng-Shou Xiao, Shengqian Ma

sqma@usf.edu

HIGHLIGHTS

Imparting superwettability on COFs via pore-surface engineering

Retained crystallinity and porosity after conferring superwettability on the COF

Improved stability of the pristine COF after being imparted with superhydrophibicity

Integration of the superhydrophobic COF with substrates to expand its application

Sun et al., Chem 4, 1726–1739
July 12, 2018
https://doi.org/10.1016/j.chempr.2018.05.020

Chem

CellPress

Article

Integrating Superwettability within Covalent Organic Frameworks for Functional Coating

Qi Sun,[1,2] Briana Aguila,[1] Jason A. Perman,[1] Taylor Butts,[1] Feng-Shou Xiao,[2] and Shengqian Ma[1,3,*]

SUMMARY

Despite the availability of a variety of skeletons for covalent organic frameworks (COFs), control of pore-surface wettability remains undeveloped, which could immensely expand their overall versatility. Herein, we contribute an effective strategy for imparting superwettability on COFs by chemically coating the pore surface with perfluoroalkyl groups to confer them with superhydrophobicity. Taking advantage of controllable modification, the resultant COFs retain the porosity and crystallinity of the pristine COFs. Benefiting from the bulk superhydrophobicity of the COF crystals and the feasibility of COF synthesis, they can be used as a coat or *in situ* integrated within various substrates; once applied, this renders them superhydrophobic. Given the modular nature, this protocol is compatible with the development of various specific wettabilities in COFs, which thereby constitutes a step for expanding the scope of COF applications and provides many opportunities for the processing of advanced materials and devices.

INTRODUCTION

Organic porous materials have technological importance and a myriad of functions and applications.[1,2] Covalent organic frameworks (COFs), an emerging class of crystalline, porous materials built from organic linkers, have rapidly grown into a major area of chemical research over the last decade.[2–10] COFs represent the development of covalent chemistry "beyond the molecule" and into extended structures,[11,12] allowing for deliberate and precise preparation of new porous materials, which have recently come into the limelight for applications in catalysis,[13–18] as promising candidates for realizing new optoelectronic-device concepts,[19] as gas storage or separation materials,[20–22] and as designable scaffolds for environmental remediation,[23] and many more are under development.[24–28] With respect to porous materials, the pore environment is of central importance for many properties given that the pore surface forms a microscopic interface with guest molecules and is a significant characteristic that determines the macroscopic nature of these materials.[29,30] In this sense, engineering the pore surface would bestow COFs with a tailor-made interface to meet specific application requirements.

Wetting is a ubiquitous phenomenon that can be observed anywhere from high tides on the beach to ion channels in cell membranes.[31–34] Controlling the wettability of solid materials presents a rational solution to combat failure related to water absorptivity and thus has attracted tremendous interest because of their potential in a broad range of fields.[35–43] For example, to protect water-sensitive metal-organic frameworks (MOFs) against decomposition in the presence of humidity,

The Bigger Picture

Wetting is a ubiquitous phenomenon that can be observed anywhere from high tides on the beach to ion channels in cell membranes. Nature has adapted over millennia to process special wettability with unique functions. Inspired by nature, artificial superhydrophobic materials have garnered widespread application. Existing coating systems for preparing superhydrophobic surfaces are predominantly confined to nonporous materials. Covalent organic frameworks (COFs), an emerging class of crystalline, porous organic materials, have rapidly grown into a major area of chemical research. Herein, we successfully impart superhydrophobicity on a COF via pore-surface engineering and a series of substrates that, after being coated with this COF, show superhydrophobicity, which greatly expands its possibilities for numerous applications. By virtue of the intrinsic properties of COFs, the composites show great promise in tackling challenges associated with energy and the environment.

functionalization with hydrophobic surfaces is an effective solution.[44–47] In addition, surface wettability control of active sites has long been used to regulate the interactions between heterogeneous catalysts and reactants and thereby the activity and selectivity.[48–50]

Despite the availability of various skeletons for COFs, engineering superwettability properties into the pore surfaces remains in its infancy.[43] It can be envisioned that imparting different superwettabilities onto COFs could allow the generation and integration of novel interfacial functional systems into devices to expand the realm of possibilities for such materials to be used in tackling current and future challenges involving energy, environment, and health.

Given the increasing demand of water-repellent materials,[51–54] here we report on an effective approach of using a facile pore-surface modification to impart the COFs with superhydrophobicity, as demonstrated by grafting fluorinated compounds onto a vinyl-functionalized COF via a thiol-ene click reaction. Through judicious choice of fluorinated compounds and careful optimization of the post-synthetic modification conditions, the resultant COF exhibits superhydrophobic behavior while retaining the porosity and crystallinity of the pristine COF. Significantly, because of the extreme water-repellent properties of superhydrophobic surfaces, virtually all aqueous liquids, including inorganic acidic and basic solutions, are prevented from permeating the material, thereby greatly improving its tolerance against variable pH environments. To show the applicability of the superhydrophobic COF, experiments were designed to integrate them with a series of substrates, including melamine foam, paper, and magnetic liquid, to confer them with superhydrophobicity. By combining the intrinsic properties of COFs and the bulk superhydrophobicity, such functional nanocoatings hold great promise to be applied as "suction skimmers" in oil-spill recovery, self-cleaning surfaces, coats for a magnetic liquid marble in microfluidic applications, and protectors for the next generation of microelectronic devices. This work therefore expands the possibilities of COFs for a plethora of target-specific applications via rational modification of pore-surface properties.

RESULTS

Synthesis of Superhydrophobic COF

To test the feasibility of pore channel engineering for controlling the wettability of COFs, we selected a COF bearing the vinyl functionality synthesized from the condensation between 1,3,5-tris(4-aminophenyl)-benzene and 2,5-divinylterephthalaldehyde, which was developed by our group, for proof of principle because of its excellent chemical stability, large pore size, and abundant high reactivity vinyl groups for potential chemical transformations (Figure 1).[23] Given the low surface free energy of fluorinated compounds,[53] especially for the long chain ones, in conjugation with the facility and controllability of the thiol-ene click reaction,[52] 1H,1H,2H,2H-perfluorodecanethiol was chosen to modify the pore surface of COF-V to manipulate the wettability. Because the enhancement of hydrophobicity, by increasing the grafting degree of fluorinated compounds, is at the expense of both porosity and crystallinity of the material, reaction conditions were screened to achieve the trade-off between hydrophobicity and the retention of intrinsic properties of the COF. Under optimal synthetic conditions, reacting COF-V with a 10% (v/v) 1H,1H,2H,2H-perfluorodecanethiol trifluorotoluene solution in the presence of a catalytic amount of azobisisobutyronitrile (AIBN) for 2 hr, resulted in the desired material (COF-VF; Figures 1 and S1). To explain the effect of the degree

[1]Department of Chemistry, University of South Florida, 4202 E. Fowler Avenue, Tampa, FL 33620, USA

[2]Key Lab of Applied Chemistry of Zhejiang Province and Department of Chemistry, Zhejiang University, Hangzhou 310028, China

[3]Lead Contact

*Correspondence: sqma@usf.edu

https://doi.org/10.1016/j.chempr.2018.05.020

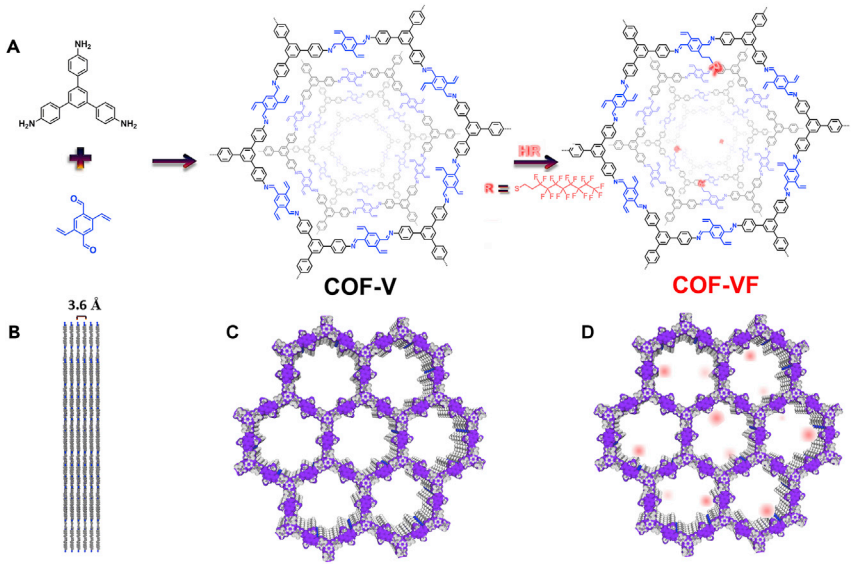

Figure 1. Schematic Illustration of Imparting Superhydrophobicity on COF-V

(A) Synthetic scheme for COF-V via condensation of 1,3,5-tris(4-aminophenyl)-benzene and 2,5-divinylterephthalaldehyde and pore-surface engineering by thiol-ene reaction with 1H,1H,2H,2H-perfluorodecanethiol.

(B and C) Side (B) and top (C) graphic views of the slipped AA stacking structure of COF-V.

(D) Graphic view of COF-VF.

See also Figures S1–S4.

of modification and the type of perfluoroalkyl group on the superhydrophobic properties of the resultant materials, we provide detailed structure-property relationships in Figures S2–S4.

Structural Characterization

Figures 2A and 2B show scanning electron microscopy (SEM) images of the COF materials before and after pore-surface modification and reveal that no noticeable morphological changes occurred and that both of them showed a large quantity of uniform nanofibers with diameters of about 80 nm. To examine the change of surface functionalities after chemical modification, we performed Fourier-transform infrared spectroscopy (FTIR), X-ray photoelectron spectroscopy (XPS), high-resolution transmission electron microscopy (TEM) energy dispersive X-ray spectroscopy (EDX) mapping, and solid-state NMR spectroscopy. The appearance of new peaks at 1,241 and 1,212 cm^{-1}, which were assigned to the C–F stretching vibration[53] together with the presence of the C–F (292.2 eV), as well as elements F (F1s at 689.6 eV) and S (S2p at 163.4 eV) signals in the FTIR (Figure S5) and XPS spectra of COF-VF (Figure S6), respectively, indicate the successful incorporation of perfluoroalkyl groups onto COF-V. The EDX mapping via TEM verifies the homogeneously distributed F, N, and S elements throughout COF-VF (Figure S7). To provide additional proof, we employed solid-state NMR analyses. As shown in Figure S8, the ^{19}F magic-angle spinning (MAS) NMR spectrum of COF-VF gave clear F signals with the same chemical shifts as those of 1H,1H,2H,2H-perfluorodecanethiol. In addition, the appearance of a noticeable peak at 26.3 ppm attributed to the alkyl carbon species from the reacted vinyl groups confirms the covalent bond formation between vinyl groups on COF-V and 1H,1H,2H,2H-perfluorodecanethiol. However, the relative intensity of the peak ascribed to the vinyl group did not change obviously in comparison with that in COF-V, suggesting that only a small part of the vinyl

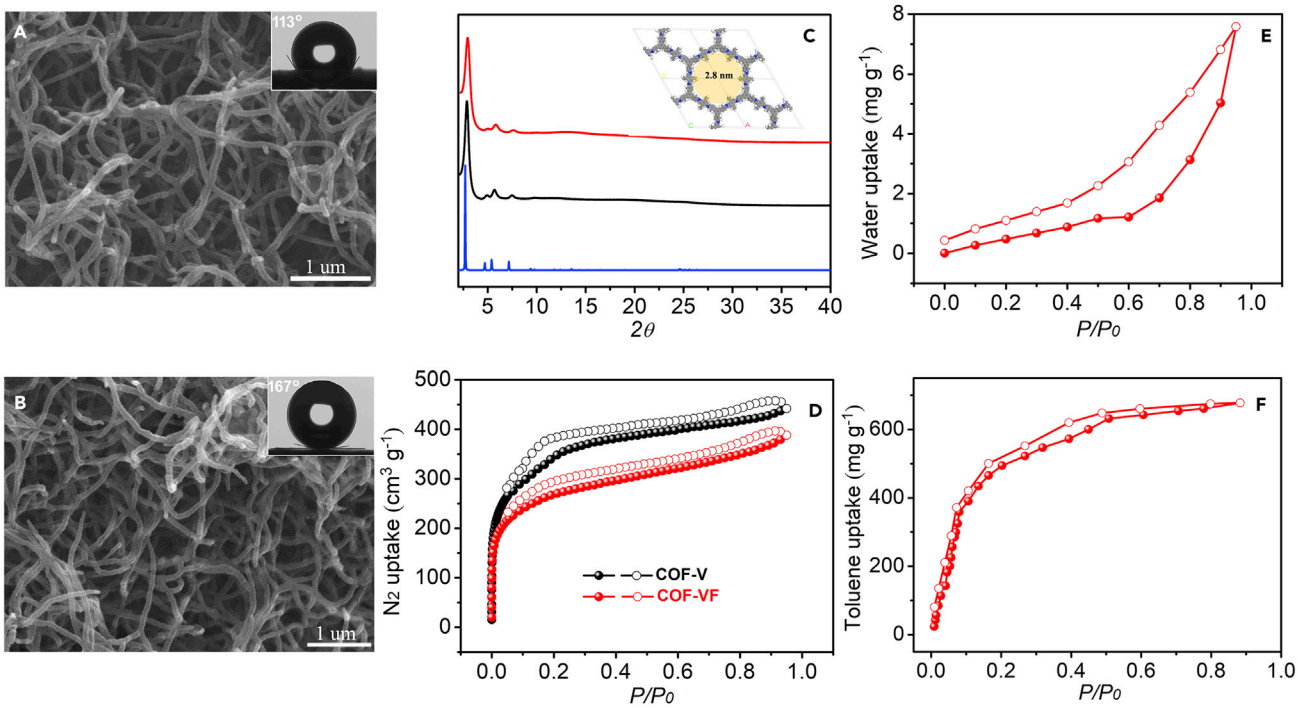

Figure 2. Structural Characterization, Wettability Tests, and Vapor Sorption Performance

(A and B) SEM images of (A) COF-V and (B) COF-VF (inset: corresponding water contact angles).

(C) PXRD profiles (inset: unit cell of the AA stacking mode of COF-V; blue, N; gray, C; white, H).

(D) Nitrogen-sorption isotherms of COF-V and COF-VF measured at 77 K.

(E) Water adsorption (solid symbols) and desorption (open symbols) isotherms of COF-VF collected at 298 K.

(F) Toluene adsorption (solid symbols) and desorption (open symbols) isotherms of COF-VF collected at 298 K.

See also Figures S5–S22.

groups participated in the reaction (Figure S9). To quantify the degree of post-synthetic modification, we evaluated the content of F species in COF-VF by elemental analysis. The results showed that the weight percentage of F species in COF-VF was 5.2 wt %, which means that about 4% of the vinyl groups were involved in the thiol-ene reaction.

To characterize the crystalline structure of COF-VF, we carried out powder X-ray diffraction (PXRD) measurements. COF-VF exhibited an intense peak at 2.8° along with some relatively weak peaks at 4.9°, 5.9°, 7.5°, and 24.9°, which agree well with the pristine pattern of COF-V, thus revealing the retention of crystallinity and structural integrity after the introduction of perfluoroalkyl groups (Figure 2C). N_2 sorption isotherms collected at 77 K showed that COF-V and COF-VF exhibited similar adsorption behavior (Figure 2D). The BET surface area of COF-VF was calculated to be as high as 938 $m^2\ g^{-1}$, rivaling that of COF-V (1,152 $m^2\ g^{-1}$), suggesting that the post-synthetic modification process has little effect on the pore structure of the pristine material and is thereby still accessible for guest molecules (see pore-size distributions of these samples in Figure S10). Thermogravimetric analysis (TGA; Figure S11) conducted in N_2 atmosphere revealed that COF-V and COF-VF exhibited very similar curves with a decomposition temperature at around 400°C, indicative of their excellent thermal stability. This was further confirmed by variable temperature PXRD, and both of them retained their crystallinity up to 300°C with decreased crystallinities observed after that (Figures S12 and S13).

Examination of Superwettability Properties

To investigate the effect of perfluoroalkyl group incorporation on the wettability of the COF material, we measured the water contact angles (CA) of the surface. COF-VF exhibited a static water CA of about 167°, thus revealing a superhydrophobic surface (superhydrophobic materials have a contact angle exceeding 150° for a water droplet; Figure 2B, inset).[52] By contrast, COF-V and COF-V modified with alkyl groups gave rise to CAs of only 113° and 122°, respectively (Figures 2A [inset] and S14, respectively). Therefore, the incorporation of perfluoroalkyl groups significantly increased the hydrophobicity. However, when oil dropped onto the surface of COF-VF, it was quickly absorbed, and COF-VF displayed a CA close to 0° (Figure S15). To further elucidate the superhydrophobicity and superoleophilicity of COF-VF, we performed vapor adsorption experiments. Water adsorption isotherms revealed that COF-VF was highly hydrophobic with a negligible water adsorption even at P/P_0 up to 0.9 (<10 mg g^{-1}), whereas COF-V exhibited a water adsorption capacity of 56 mg g^{-1} (Figure S16). In contrast, it had a toluene adsorption isotherm that showed a sharp uptake at very low pressure ($P/P_0 < 0.1$) and attained a saturation capacity exceeding 680 mg g^{-1} at $P/P_0 = 0.88$. To further investigate the impact by introducing fluorine species on the materials' affinity toward H_2O and oil, we collected sorption isotherms of COF-V and COF-VF for H_2O and toluene and compared them at 298 and 323 K (Figures S17–S19). COF-VF exhibited a higher affinity toward toluene and a lower affinity to H_2O in relation to COF-V. These results indicate that the large channels in COF-VF are restricted to water yet permitted to toluene and exhibit superior hydrophobic and oleophilic behaviors, which offer exceptional abilities to overcome the problems associated with the adsorption of harmful volatile organic compounds in humid environments.

Investigation of the Chemical Shielding Effect

Given the importance of chemical stability for practical applications, the tolerance of COF-VF under a wide range of conditions was tested. Notably, after 1 week of treatment in 12 M HCl and 14 M NaOH at room temperature, as well as boiling water, COF-VF still retained its crystallinity and porosity (Figures S20 and S21). To further evaluate the chemical shielding effect resulting from superhydrophobicity, we monitored the PXRD patterns of COF-VF exposed to 100% relative humidity under HCl or NH_3 atmosphere at room temperature. COF-VF did not show noticeable change in the PXRD patterns, even after aging under the above conditions over 48 hr (Figure S20). In sharp contrast, COF-V could not survive in 2 M HCl or a humid HCl gas atmosphere after suspension and exposure for only 12 hr (Figure S22). These results indicate that hydrophobic modifications to the COF material can appreciably safeguard the crystallinity. We attribute the observed ultrastability of COF-VF toward acid and base to the extreme water-repellent properties of superhydrophobic surfaces, which serve as chemical shields to prevent the permeation of acidic and basic aqueous solutions.

Integration of the Superhydrophobic COF and Melamine Foam for Oil Recovery

By embracing the features of superhydrophobicity and superoleophilicity together with high porosity and chemical stability, COF-VF could be beneficial in mitigating environmental problems caused by the release of harmful organic compounds. However, COF-VF was synthesized as a microcrystalline powder, and therefore its applications in real-world separation could be affected by poor processability and handling.[55] In addition, the limited pore volume of the COF material restricts the adsorption capacity. In this context, we were motivated to incorporate superhydrophobic COF coatings onto other substrates to add applicability. Of the various

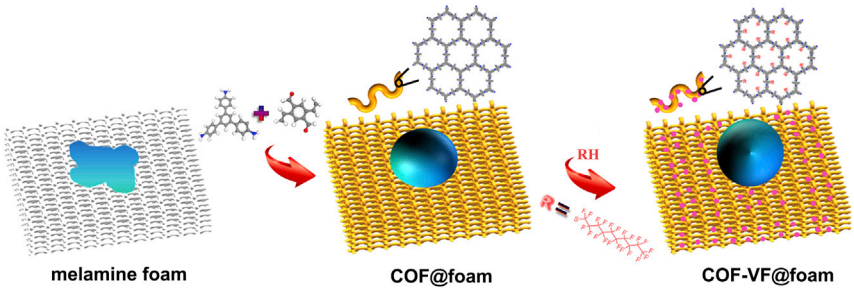

Figure 3. Schematic Illustration of the Preparation of Superhydrophobic COF-VF-Coated Melamine Foam (COF-VF@foam)

See also Figures S23–S27.

supports, melamine foams have several appealing features on account of their high chemical and mechanical stability, large void fractions, and unique structure, which offers binding affinity for the growth and anchoring of COF microcrystals by π-π interaction and hydrogen bonding.[56] To increase the interaction between the melamine foam and the COF to realize the homogeneous distribution of the COF throughout the foam, we employed a bottom-up synthetic pathway for COF immobilization on the foam for potential application in process-intensive systems. Monolithic melamine foam was submerged in a solution of the monomers and catalyst (acetic acid) for COF synthesis. Upon being heated at 100°C for 3 days and then treated with 1H,1H,2H,2H-perfluorodecanethiol, the foam exhibited a homogeneous color change from white to light yellow, suggesting that the monolithic foam was coated and interpenetrated by the COF (Figure 3).

SEM images of the bare and COF-coated melamine foam (Figures S23 and S24) show that the microstructure of the foam remained unchanged, but further magnification reveals a distinctive difference in the surface morphology. The smooth melamine framework was encased by the COF products, which resulted in a surface roughness as shown in Figure S24. Furthermore, the presence of strong signals associated with the C–F stretching vibration, as well as S and F species in the FTIR and XPS spectra of COF-VF@foam, respectively, confirms the incorporation of COF-VF onto the melamine foam (Figures S25–S27). More importantly, the coating of the COF onto the surface of the skeletons turned the foam from hydrophilic to hydrophobic. Figure 4A depicts a photograph of COF-VF@foam floating atop a water bath while the pristine melamine foam sits at the bottom. When COF-VF@foam was immersed in water by an external force, an interface formed between entrapped air residing along the surface of the foam and the surrounding water, giving rise to a mirror-like surface on COF-VF@foam; this phenomenon was due to the Cassie-Baxter nonwetting behavior (Figure 4B).[57] After the external force was released, COF-VF@foam immediately floated to the water surface without absorbing any of the surrounding water, indicating its excellent water repellency. The hydrophobicity of COF-VF@foam was characterized by water CA measurements. As displayed in Figure 4C, the water CA of COF-VF@foam was as high as 152°, confirming the superhydrophobic characteristics of the functionalized foam. To examine the wetting behavior of oil on COF-VF@foam, we dropped nitrobenzene (10 μL) on the membrane surface; it spread out quickly, and a nearly zero CA was reached (Figure S28). These results indicate that COF-VF@foam also exhibits superhydrophobic and superoleophilic properties. Notably, unlike many previous superhydrophobic foams in which hydrophobic coatings are physically attached onto the external surface of the foam and easily detached, the COF powders are wrapped throughout the

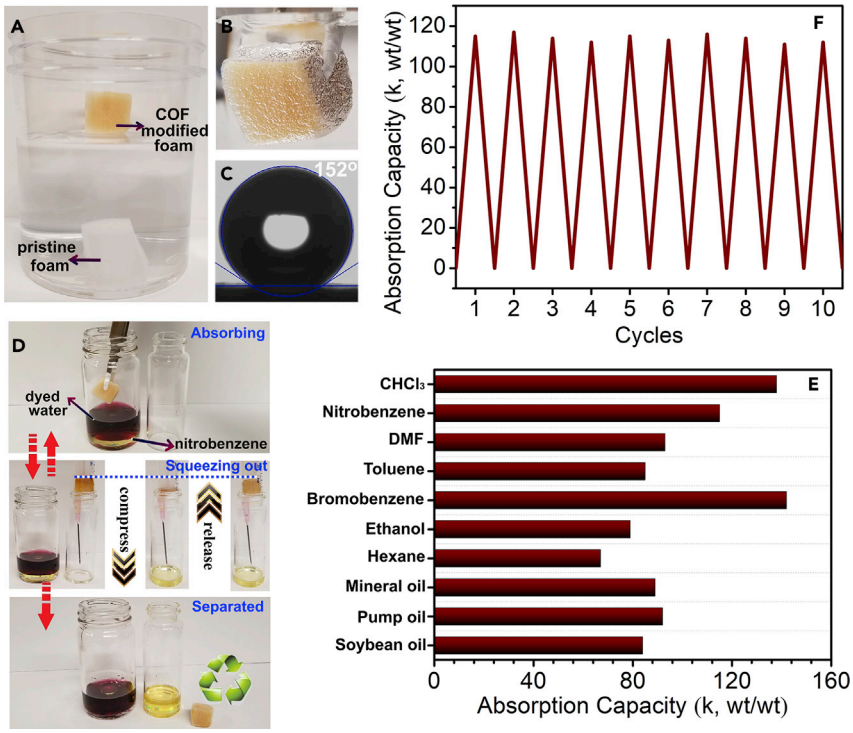

Figure 4. Superhydrophobic Property and Oil-Sorption Performance Tests

(A) Photograph of COF-VF@foam (yellow) and melamine foam (white) after being placed on water.

(B) Photograph of COF-VF@foam immersed in water by a force.

(C) Water contact angle on the surface of COF-VF@foam.

(D) COF-VF@foam can separate underwater oil such as nitrobenzene from water (see also Video S1).

(E) Absorption capacities of COF-VF@foam for various organic solvents and oils, as indicated by weight gain.

(F) Weight gain during nitrobenzene absorption and squeezing cycles.

See also Figures S28 and S29, and Table S1.

skeletons, which remain unaffected by the squeezing process.[57] The mechanical stability of the melamine foam was retained during the coating processes, during which COF-VF@foam was subjected to compression and distortion and displayed elastomer characteristics (Figure S29). The combination of flexibility and superhydrophobicity and superoleophilicity allows COF-VF@foam to be used directly as a compressible adsorbent for simple removal of organic pollutants. We therefore investigated its potential to clean up oil spills. Given the challenge to clean up underwater oil, nitrobenzene and 0.25 wt % Arsenazo III aqueous solution were poured into a vial to clearly distinguish the nitrobenzene phase from the water. When COF-VF@foam was inserted into the vial, nitrobenzene below the water was efficiently removed, and the pristine melamine foam absorbed only the aqueous solution (see also Video S2). Importantly, the oil-absorption kinetics of COF-VF@foam was very rapid, and the foam reached its saturated absorption capacity within 5 s, as seen in Video S1, and the captured oil was readily removed by simple squeezing of the foam; the recovered COF-VF@foam was reused without any loss in its performance, thus suggesting that COF-VF@foam is a promising candidate as a "suction skimmer" in marine oil-spill recovery (Figure 4D). To investigate the maximum sorption capacity, we performed sorption tests in organic solvents and oils in the absence of water. The oil absorption capacity of COF-VF@foam was calculated by the following equation: absorption capacity (κ) = $(m_s - m_0)/m_0$, where m_s

and m_0 indicate the weight of COF-VF@foam before and after oil absorption, respectively; the absorption capacity of the tested solvents is represented in Figure 4E. Various organic solvents and oils with different polarities, densities, and viscosities were tested. COF-VF@foam exhibited remarkable sorption capacities from 67 to 142 times its own weight, placing it within striking distance of the all-time oil-uptake record (Table S1).[57–65] The absorption capacity of COF-VF@foam increased as a function of the solvent density given that the pore volume for bulk solvent storage was mainly provided by the micrometer-sized pores of the melamine foam. More interestingly, COF-VF@foam also showed excellent recyclability with sorption capacity retention after ten cycles of sorption squeezing of more than 93% for multiple organic solvents and oils, thus validating its great potential in water remediation (Figure 4F).

COF-VF as a Nanocoat for Various Substrates

Currently, the creation of a superhydrophobic surface has stimulated great interest for both fundamental research and practical applications.[51] Given the bulk superhydrophobicity of COF-VF powders, it should be useful in conferring superhydrophobicity to any arbitrary surface to which it is applied. To test this concept, we sprayed the COF-VF powder onto adhesive tape, and the resultant surface was seemingly impervious to water and concentrated aqueous acid or base. After application, the droplets completely rolled off the surface without wetting or contaminating the surface (Figure S30 and see also Video S3). It is worth pointing out that our superhydrophobic layers encompass the entire thickness, and they are able to display significant durability. When the top layer is damaged, the underlying structure becomes exposed and the surface remains superhydrophobic. This improves upon other methods developed for fabricating superhydrophobic surfaces on the basis of the generation of roughness; these surfaces are easily destroyed when they are scratched or even pressed. To prove this statement and highlight the importance of bulky superhydrophobicity of the material for the maintenance of long-term stability, we compared the stability of the materials' hydrophobicity as a result of chemical composition and microstructure, as exemplified by COF-VF and nickel foam, respectively. The superhydrophobicity of COF-VF was retained after we exerted pressure, whereas the hydrophobic nickel foam became hydrophilic as a result of the loss of roughness (Figure S31).

To further demonstrate that the ultrastability of superhydrophobicity originated from chemical modification, we physically mixed COF-V and 1H,1H,2H,2H-perfluorodecanethiol at a mass ratio of 100/8 so that the mixture (COF-V&F) had the same amount of F as COF-VF. CA test results revealed that COF-V&F had a higher CA (as high as 138°) than COF-V (Figure S32). However, it was still below the range of superhydrophobicity, partly because the F species was less homogeneous than chemical grafting. More importantly, the increased hydrophobicity was not stable, and after rinsing with organic solvents, a comparison of the waterproof properties of coating onto adhesive tape before and after soaking in acetone revealed that such improvement disappeared. The water droplets completely rolled off the surface without wetting or contaminating the freshly made surface, whereas water drops very easily stuck on the rinsed surface (Video S4).

Apart from conferring the solid substrates with superhydrophobicity, COF-VF is also applicable to aqueous solutions to form liquid marbles, which are of potential benefit in microfluidic applications and also permit the study of a drop in a nonwetting situation.[66–68] In particular, magnetic liquid marbles have recently attracted

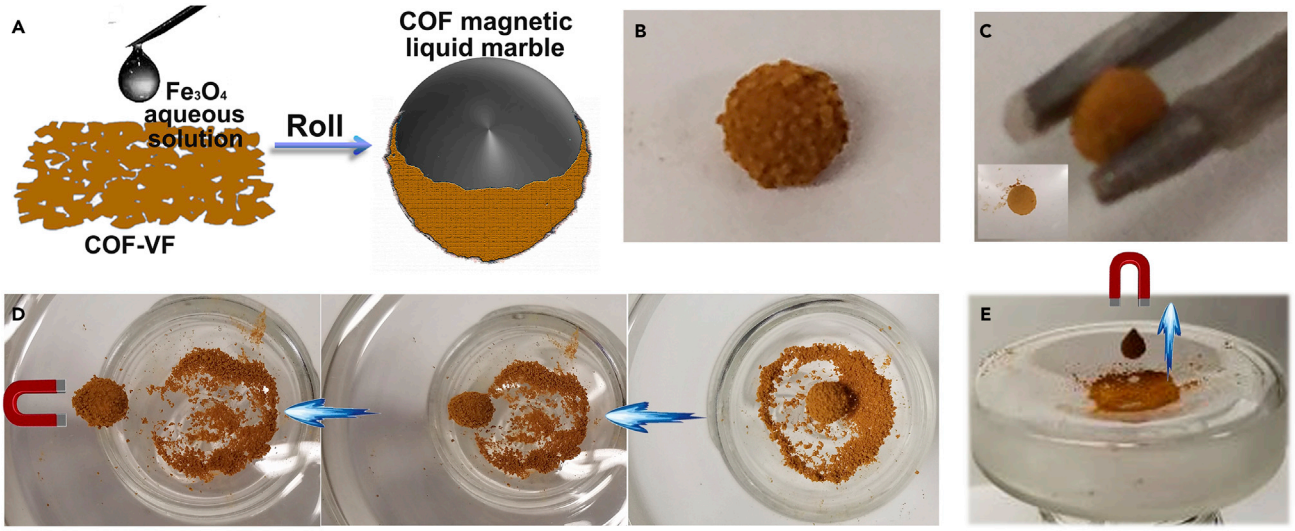

Figure 5. Superhydrophobic Coat

(A) Schematic illustration of the preparation of COF magnetic liquid marbles.

(B) Photograph of a COF magnetic liquid marble made from 0.1 mL of Fe_3O_4 aqueous solution placed on a glass plate.

(C) Photograph of a COF magnetic liquid marble picked up by a pair of tweezers and then transferred onto a water surface in a Petri dish (inset).

(D) Magnetic actuation of a liquid marble with movement from right to left over an upslope.

(E) Magnetic actuation of a liquid marble with movement up and down.

See also Figure S33.

extensive attention because of their magnet responsive ability.[69,70] To demonstrate this concept, we encapsulated an aqueous solution of Fe_3O_4 nanoparticles into COF powders. As schematically shown in Figure 5A, we readily obtained the magnetic liquid marbles by rolling water droplets on a pile of superhydrophobic COF powders. As the water droplet was rolled over, the COF powders, behaving like a soft solid, spontaneously self-organized to encapsulate the water droplet and render the droplet nonwetting to the substrate. The spontaneous attachment of the nanoparticles at the liquid-air interface can be understood by the minimization of the free energy of the surface. Figure 5B shows a typical digital photograph of a liquid marble prepared from 0.1 mL of water (containing 2 wt % Fe_3O_4), which could roll freely on the surface of a glass plate. The mechanical robustness of the resultant magnetic liquid marbles was demonstrated by impact deformation and marble rebound, which is an essential requirement for their applications in microfluidic devices. The excellent stability of the liquid marble is further supported by its capability to be handled with a pair of tweezers without breaking, and the liquid marble remained intact after being transferred onto a water surface in a Petri dish (Figure 5C). Driven by a magnetic bar, the direction of the liquid marble's movement changed in response to the motion of the external magnet. The liquid marble could be transported not only on flat surfaces but also on upslope surfaces and jump up and down in a curve (as illustrated in Figures 5D and 5E), which will facilitate the generation of topologically complex microfluidic systems. Given the inherent porosity of COF-VF, the superhydrophobic shell of a liquid marble allows gas transport but prevents contact between its liquid core and outside surfaces. These properties intuitively enable them to be used as a gas or vapor sensor, and liquid marbles loaded with different indicators can simultaneously sense different gases via different mechanisms. To highlight the advantage of a porous material (like COFs) over other organic superhydrophobic materials, we made side-by-side comparisons with liquid marbles formed by nonporous polytetrafluoroethylene. We carried out ammonia

sensing from an aqueous NH_3-emitting source by using liquid marbles. Liquid marbles loaded with phenolphthalein or transition-metal salt ($CoCl_2$) indicator were placed onto the surface of a NH_4OH solution (2 wt %). Rapid color changes of liquid marbles made of COF-VF were observed (within 1 min), whereas no noticeable changes were detected for those with nonporous polytetrafluoroethylene under identical conditions, indicative of the superiority of porous materials as a permeable shell (Figure S33).

DISCUSSION

In summary, we have determined that pore-surface modification of COFs serves as an excellent approach to improving applicability of these materials. This study demonstrates the successful impartment of a COF material with superhydrophobicity and its potential applications by integrating it with other substrates, such as melamine foam and magnetic liquids. This proof-of-concept study is an important first step toward exploiting new capabilities for COF materials by combining them with superwettability. Fundamentally, it expands the superwettability control space that can be carried out within COFs as an emerging class of porous crystalline materials to more than just 2D surfaces.

This work highlights the opportunity to design smart materials by taking advantage of the ability to synergistically integrate multiple functionalities into COFs. In addition to sharing the attributes of general superhydrophobic surfaces, such as self-cleaning and waterproofing, the surfaces created by the COFs are expected to possess other unique functions as a result of the intrinsic properties of COFs, which hold great promise in applications such as wearable microelectronic devices. For example, unlike many other nonporous coatings, which provide a nonbreathable layer, the pores of COFs are permeable to air, thus facilitating the release of the heat generated by electronic devices as well as aiding in the comfort of functional garments. Considering the tunable synthesis of COFs and the modular nature of surface properties in conjunction with the compatibility of the resultant COF materials to integrate with a variety of substrates, our work therefore opens a new avenue for the task-specific application of COFs.

EXPERIMENTAL PROCEDURES

Materials

Commercially available reagents were purchased in high purity and used without purification. Solvents were purified according to standard laboratory methods.

Synthesis of COF-VF

10% v/v 1H,1H,2H,2H-perfluorodecanethiol trifluorotoluene solution (10 mL) was introduced to a mixture of COF-V (100 mg), which was synthesized as described in the literature,[23] and a catalytic amount of azobisisobutyronitrile (AIBN). After being stirred at 60°C for 2 hr, the title product was isolated by filtration, washed with acetone, and dried under vacuum at 50°C.

Synthesis of COF-VF@foam

Melamine foam (ca. 3 mg) was soaked in a mixture of 1,3,5-tris(4-aminophenyl)-benzene (4 mg) and 2,5-divinylterephthalaldehyde (3 mg) in anisole (4.75 mL) and phenethanol (0.25 mL) for 24 hr. Then, 0.5 mL of 6 M aqueous acetic acid was added, and the tube was flash frozen at 77 K, evacuated, and sealed. The reaction mixture was heated at 100°C for 3 days, and the resultant foam was washed thoroughly with acetone and dried under vacuum. The dried foam was

then soaked in 10% v/v 1H,1H,2H,2H-perfluorodecanethiol trifluorotoluene solution (10 mL) with a catalytic amount of azobisisobutyronitrile (AIBN) and heated at 60°C for 24 hr. The title product was isolated, washed with acetone, and dried under vacuum at 50°C. The COF weight percent in the resultant COF-VF@foam was around 10 wt %, calculated on the basis of the mass increase after the COF material was introduced. To homogeneously integrate COF-V with melamine foam, we modified the COF-V synthesis conditions. Under these conditions, the system is homogeneous before heating, which is essential for the resulting COF-V crystals to uniformly wrap the foam fibers. The SEM image and XRD pattern of COF-V synthesized under these conditions in the absence of melamine foam are shown in Figure S34 for comparison. To check the crystallinity of the COF-VF component on COF-VF@foam, we tested the XRD of the fine ground composite, which exhibited obvious diffraction peaks, thus indicting the crystallinity of the COF-VF component in COF-VF@foam (Figure S35). The relatively weak peaks observed can be reasonably attributed to the fact that COF-VF takes up only a very small fraction of the COF-VF@foam composite.

Characterization

Infrared spectra were recorded on a Nicolet Impact 410 FTIR spectrometer. Inductively coupled plasma-optical omission spectrometry was performed on a PerkinElmer Elan DRC II Quadrupole. XPS was performed on a Thermo ESCALAB 250 with Al Kα irradiation at $\theta = 90^{\circ}$ for X-ray sources, and the binding energies were calibrated with the C1s peak at 284.9 eV. ^{1}H NMR spectra were recorded on a Bruker Avance-400 (400 MHz) spectrometer. Chemical shifts are expressed in ppm downfield from tetramethylsilane at $\delta = 0$ ppm, and J values are given in Hz. ^{13}C and ^{19}F cross-polarization MAS was recorded on a Varian infinity plus 400 spectrometer equipped with a magic-angle spin probe in a 4-mm ZrO_2 rotor. PXRD data were collected on a Bruker AXS D8 Advance A25 powder X-ray diffractometer (40 kV, 40 mA) with Cu Kα ($\lambda = 1.5406$ Å) radiation. Variable temperature X-ray diffraction patterns were recorded from 298 to 673 K with a heating rate of 10°C min^{-1} under ambient conditions. The gas adsorption isotherms were collected on a surface-area analyzer (ASAP 2020). The N_2 sorption isotherms were measured at 77 K in a liquid N_2 bath. SEM images were collected with a Hitachi SU 1510. Photographs of water and organic compounds on the surface of the samples in the pressed pellet form were measured with SL200KB (USA KNO Industry), equipped with a charge-coupled device camera. Water adsorption and desorption isotherms were obtained via SMS Instruments DVS Advantage. The balance has a sensitivity of 0.1 mg. We measured these isotherms at 298 K by monitoring the weight change of the sample as a function of the relative humidity of water. The relative humidity of water was stepped up from 0% to 98% with an increment of 10% at each step and was then stepped down to 0%. Real-time weight, temperature, and relative humidity were recorded. Toluene adsorption isotherms were measured via Micromeritics 3Flex. We collected these isotherms at 298 K by monitoring the volume change. TGA was carried out on a Q50 thermogravimetric analyzer under a N_2 atmosphere. High-angle annular dark-field scanning, scanning TEM imaging, and EDX mapping were carried out by Titan ChemiSTEM operated at 200 kV.

SUPPLEMENTAL INFORMATION

Supplemental Information includes 35 figures, 1 table, and 4 videos and can be found with this article online at https://doi.org/10.1016/j.chempr.2018.05.020.

ACKNOWLEDGMENTS

The authors acknowledge the US National Science Foundation (CBET-1706025) and the University of South Florida for financial support of this work. The National Natural Science Foundation of China (21720102001) is also acknowledged.

AUTHOR CONTRIBUTIONS

Q.S. and S.M. conceived and designed the research. Q.S., B.A., J.A.P., and S.M. drafted the manuscript. Q.S., B.A., and T.B. carried out the experiments. F.-S.X. assisted with additional experiments and participated in discussions. All authors discussed the results and approved the final version of the manuscript.

DECLARATION OF INTERESTS

The authors declare no competing interests.

Received: February 15, 2018
Revised: April 10, 2018
Accepted: May 25, 2018
Published: June 21, 2018

REFERENCES AND NOTES

1. Slater, A.G., and Cooper, A.I. (2015). Function-led design of new porous materials. Science *348*, aaa8075.
2. Das, S., Heasman, P., Ben, T., and Qiu, S. (2017). Porous organic materials: strategic design and structure-function correlation. Chem. Rev. *117*, 1515–1563.
3. Côté, A.P., Benin, A.I., Ockwig, N.W., O'Keeffe, M., Matzger, A.J., and Yaghi, O.M. (2005). Porous, crystalline, covalent organic frameworks. Science *310*, 1166–1170.
4. Feng, X., Ding, X., and Jiang, D. (2012). Covalent organic frameworks. Chem. Soc. Rev. *41*, 6010–6022.
5. Ding, S.-Y., and Wang, W. (2013). Covalent organic frameworks (COFs): from design to applications. Chem. Soc. Rev. *42*, 548–568.
6. Ascherl, L., Sick, T., Margraf, J.T., Lapidus, S.H., Calik, M., Hettstedt, C., Karaghiosoff, K., Döblinger, M., Clark, T., Chapman, K.W., et al. (2016). Molecular docking sites designed for the generation of highly crystalline covalent organic frameworks. Nat. Chem. *8*, 310–316.
7. Kandambeth, S., Mallick, A., Lukose, B., Mane, M.V., Heine, T., and Banerjee, R. (2012). Construction of crystalline 2D covalent organic frameworks with remarkable chemical (acid/base) stability via a combined reversible and irreversible route. J. Am. Chem. Soc. *134*, 19524–19527.
8. Pang, Z.-F., Xu, S.-Q., Zhou, T.-Y., Liang, R.-R., Zhan, T.-G., and Zhao, X. (2016). Construction of covalent organic frameworks bearing three different kinds of pores through the heterostructural mixed linker strategy. J. Am. Chem. Soc. *138*, 4710–4713.
9. Lanni, L.M., Tilford, R.W., Bharathy, M., and Lavigne, J.J. (2011). Enhanced hydrolytic stability of self-assembling alkylated two-dimensional covalent organic frameworks. J. Am. Chem. Soc. *133*, 13975–13983.
10. Bunck, D.N., and Dichtel, W.R. (2012). Functionalization of three-dimensional covalent organic frameworks. Angew. Chem. Int. Ed. *51*, 1885–1889.
11. Jiang, J., Zhao, Y., and Yaghi, O.M. (2016). Covalent chemistry beyond molecules. J. Am. Chem. Soc. *138*, 3255–3265.
12. Diercks, C.S., and Yaghi, O.M. (2017). The atom, the molecule, and the covalent organic framework. Science *355*, https://doi.org/10.1126/science.aal1585.
13. Xu, H., Gao, J., and Jiang, D. (2015). Stable, crystalline, porous, covalent organic frameworks as a platform for chiral organocatalysts. Nat. Chem. *7*, 905–912.
14. Ding, S.-Y., Gao, J., Wang, Q., Zhang, Y., Song, W.-G., Su, C.-Y., and Wang, W. (2011). Construction of covalent organic framework for catalysis: Pd/COF-LZU1 in Suzuki-Miyaura coupling reaction. J. Am. Chem. Soc. *133*, 19816–19822.
15. Fang, Q., Gu, S., Zheng, J., Zhuang, Z., Qiu, S., and Yan, Y. (2014). 3D microporous base-functionalized covalent organic frameworks for size-selective catalysis. Angew. Chem. Int. Ed. *53*, 2878–2882.
16. Vyas, V.S., Haase, F., Stegbauer, L., Savasci, G., Podjaski, F., Ochsenfeld, C., and Lotsch, B.V. (2015). A tunable azine covalent organic framework platform for visible light-induced hydrogen generation. Nat. Commun. *6*, 8508.
17. Sun, Q., Aguila, B., Perman, J.A., Nguyen, N., and Ma, S. (2016). Flexibility matters: cooperative active sites in covalent organic framework and threaded ionic polymer. J. Am. Chem. Soc. *138*, 15790–15796.
18. Wang, X., Han, X., Zhang, J., Wu, X., Liu, Y., and Cui, Y. (2016). Homochiral 2D porous covalent organic frameworks for heterogeneous asymmetric catalysis. J. Am. Chem. Soc. *138*, 12332–12335.
19. Bertrand, G.H.V., Michaelis, V.K., Ong, T.-C., Griffin, R.G., and Dincă, M. (2013). Thiophene-based covalent organic frameworks. Proc. Natl. Acad. Sci. USA *110*, 4923–4928.
20. Du, Y., Yang, H., Whiteley, J.M., Wan, S., Jin, Y., Lee, S.-H., and Zhang, W. (2016). Ionic covalent organic frameworks with spiroborate linkage. Angew. Chem. Int. Ed. *55*, 1737–1741.
21. Zeng, Y., Zou, R., and Zhao, Y. (2016). Covalent organic frameworks for CO_2 capture. Adv. Mater. *28*, 2855–2873.
22. Baldwin, L.A., Crowe, J.W., Pyles, D.A., and McGrier, P.L. (2016). Metalation of a mesoporous three-dimensional covalent organic framework. J. Am. Chem. Soc. *138*, 15134–15137.
23. Sun, Q., Aguila, B., Perman, J., Earl, L., Abney, C., Cheng, Y., Wei, H., Nguyen, N., Wojtas, L., and Ma, S. (2017). Postsynthetically modified covalent organic frameworks for efficient and effective mercury removal. J. Am. Chem. Soc. *139*, 2786–2793.
24. Fang, Q., Wang, J., Gu, S., Kaspar, R.B., Zhuang, Z., Zheng, J., Guo, H., Qiu, S., and Yan, Y. (2015). 3D porous crystalline polyimide covalent organic frameworks for drug delivery. J. Am. Chem. Soc. *137*, 8352–8355.
25. Kandambeth, S., Venkatesh, V., Shinde, D.B., Kumari, S., Halder, A., Verma, S., and Banerjee, R. (2015). Self-templated chemically stable hollow spherical covalent organic framework. Nat. Commun. *6*, 6786.
26. Ma, H., Liu, B., Li, B., Zhang, L., Li, Y.-G., Tan, H.-Q., Zang, H.-Y., and Zhu, G. (2016). Cationic covalent organic frameworks: a simple platform of anionic exchange for porosity tuning and proton conduction. J. Am. Chem. Soc. *138*, 5897–5903.
27. Wang, S., Wang, Q., Shao, P., Han, Y., Gao, X., Ma, L., Yuan, S., Ma, X., Zhou, J., Feng, X., and Wang, B. (2017). Exfoliation of covalent organic

frameworks into few-layer redox-active nanosheets as cathode materials for lithium-ion batteries. J. Am. Chem. Soc. *139*, 4258–4261.

28. Qian, H.-L., Yang, C.-X., and Yan, X.-P. (2016). Bottom-up synthesis of chiral covalent organic frameworks and their bound capillaries for chiral separation. Nat. Commun. *7*, 12104.

29. Nagai, A., Guo, Z., Feng, X., Jin, S., Chen, X., Ding, X., and Jiang, D. (2011). Pore surface engineering in covalent organic frameworks. Nat. Commun. *2*, 536.

30. Jiang, H.-L., Feng, D., Liu, T.-F., Li, J.R., and Zhou, H.-C. (2012). Pore surface engineering with controlled loadings of functional groups via click chemistry in highly stable metal-organic frameworks. J. Am. Chem. Soc. *134*, 14690–14693.

31. Su, B., Tian, Y., and Jiang, L. (2016). Bioinspired interfaces with superwettability: from materials to chemistry. J. Am. Chem. Soc. *138*, 1727–1748.

32. Bellanger, H., Darmanin, T., de Givenchy, E.T., and Guittard, F. (2014). Chemical and physical pathways for the preparation of superoleophobic surfaces and related wetting theories. Chem. Rev. *114*, 2694–2716.

33. Li, X.-M., Reinhoudt, D., and Crego-Calama, M. (2007). What do we need for a superhydrophobic surface? A review on the recent progress in the preparation of superhydrophobic surfaces. Chem. Soc. Rev. *36*, 1350–1368.

34. Zhang, C., Mcadams, D.A., and Grunlan, J.C. (2016). Nano/micro-manufacturing of bioinspired materials: a review of methods to mimic natural structures. Adv. Mater. *28*, 6292–6321.

35. Yao, X., Song, Y., and Jiang, L. (2011). Applications of bio-inspired special wettable surfaces. Adv. Mater. *23*, 719–734.

36. Jayaramulu, K., Datta, K.K.R., Rösler, C., Petr, M., Otyepka, M., Zboril, R., and Fischer, R.A. (2016). Biomimetic superhydrophobic/superoleophilic highly fluorinated graphene oxide and ZIF-8 composites for oil-water separation. Angew. Chem. Int. Ed. *55*, 1178–1182.

37. Yuan, J., Liu, X., Akbulut, O., Hu, J., Suib, S.L., Kong, J., and Stellacci, F. (2008). Superwetting nanowire membranes for selective absorption. Nat. Nanotechnol. *3*, 332–336.

38. Pan, S., Kota, A.K., Mabry, J.M., and Tuteja, A. (2013). Superomniphobic surfaces for effective chemical shielding. J. Am. Chem. Soc. *135*, 578–581.

39. Tian, X., Shaw, S., Lind, K.R., and Cademartiri, L. (2016). Thermal processing of silicones for green, scalable, and healable superhydrophobic coatings. Adv. Mater. *28*, 3677–3682.

40. Mullangi, D., Shalini, S., Nandi, S., Choksi, B., and Vaidhyanathan, R. (2017). Super-hydrophobic covalent organic frameworks for chemical resistant coatings and hydrophobic paper and textile composites. J. Mater. Chem. A *5*, 8376–8384.

41. Yang, C., Kaipa, U., Mather, Q.Z., Wang, X., Nesterov, V., Venero, A.F., and Omary, M.A. (2011). Fluorous metal-organic frameworks with superior adsorption and hydrophobic properties toward oil spill cleanup and hydrocarbon storage. J. Am. Chem. Soc. *133*, 18094–18097.

42. Padial, N.M., Procopio, E.Q., Montoro, C., López, E., Oltra, J.E., Colombo, V., Maspero, A., Masciocchi, N., Galli, S., Senkovska, I., et al. (2013). Highly hydrophobic isoreticular porous metal-organic frameworks for the capture of harmful volatile organic compounds. Angew. Chem. Int. Ed. *52*, 8290–8294.

43. Mitra, S., Sasmal, H.S., Kundu, T., Kandambeth, S., Illath, K., Díaz, D.D., and Banerjee, R. (2017). Drug delivery in covalent organic nanosheets (CONs) via sequential postsynthetic modification. J. Am. Chem. Soc. *139*, 4513–4520.

44. Sun, Q., He, H., Gao, W.-Y., Aguila, B., Wojtas, L., Dai, Z., Li, J., Chen, Y.-S., Xiao, F.-S., and Ma, S. (2016). Imparting amphiphobicity on single-crystalline porous materials. Nat. Commun. *7*, 13300.

45. Zhang, W., Hu, Y., Ge, J., Jiang, H.-L., and Yu, S.-H. (2014). A facile and general coating approach to moisture/water-resistant metal-organic frameworks with intact porosity. J. Am. Chem. Soc. *136*, 16978–16981.

46. Nguyen, J.G., and Cohen, S.M. (2010). Moisture-resistant and superhydrophobic metal-organic frameworks obtained via postsynthetic modification. J. Am. Chem. Soc. *132*, 4560–4561.

47. McGuire, C.V., and Forgan, R.S. (2015). The surface chemistry of metal-organic frameworks. Chem. Commun. *51*, 5199–5217.

48. Sun, Q., Aguila, B., Verma, G., Liu, X., Dai, Z., Deng, F., Meng, X., Xiao, F.-S., and Ma, S. (2016). Superhydrophobicity: constructing homogeneous catalysts into superhydrophobic porous frameworks to protect them from hydrolytic degradation. Chem *1*, 628–639.

49. Huang, G., Yang, Q., Xu, Q., Yu, S.-H., and Jiang, H.-L. (2016). Polydimethylsiloxane coating for a palladium/MOF composite: highly improved catalytic performance by surface hydrophobization. Angew. Chem. Int. Ed. *55*, 7379–7383.

50. Yuan, C., Luo, W., Zhong, L., Deng, H., Liu, J., Xu, Y., and Dai, L. (2011). Gold@ polymer nanostructures with tunable permeability shells for selective catalysis. Angew. Chem. Int. Ed. *50*, 3155–3159.

51. Levkin, P.A., Svec, F., and Fréchet, M.J. (2009). Porous polymer coatings: a versatile approach to superhydrophobic surfaces. Adv. Funct. Mater. *19*, 1993–1998.

52. Darmanin, T., and Guittard, F. (2014). Recent advances in the potential applications of bioinspired superhydrophobic materials. J. Mater. Chem. A *2*, 16319–16359.

53. Hayase, G., Kanamori, K., Hasegawa, G., Maeno, A., Kaji, H., and Nakanishi, K. (2013). A superamphiphobic macroporous silicone monolith with marshmallow-like flexibility. Angew. Chem. Int. Ed. *52*, 10788–10791.

54. Zhou, H., Wang, H., Niu, H., Zhao, Y., Xu, Z., and Lin, T. (2017). A waterborne coating system for preparing robust, self-healing, superamphiphobic surfaces. Adv. Funct. Mater. https://doi.org/10.1002/adfm.201604261.

55. Kandambeth, S., Biswal, B.P., Chaudhari, H.D., Rout, K.C., Kunjattu, H.S., Mitra, S., Karak, S., Das, A., Mukherjee, R., et al. (2017). Selective molecular sieving in self-standing porous covalent-organic-framework membranes. Adv. Mater. *29*, 1603945.

56. Wu, Y., Guo, J., and Wang, C. (2016). An elastic monolithic catalyst: a microporous metalloporphyrin-containing framework-wrapped melamine foam for process-intensified acyl transfer. Angew. Chem. Int. Ed. *55*, 6013–6017.

57. Nguyen, D.D., Tai, N.-H., Lee, S.-B., and Kuo, W.-S. (2012). Superhydrophobic and superoleophilic properties of graphene-based sponges fabricated using a facile dip coating method. Energy Environ. Sci. *5*, 7908–7912.

58. Kim, D., Kim, D.W., Buyukcakir, O., Kim, M.-K., Polychronopoulou, K., and Coskun, A. (2017). Highly hydrophobic ZIF-8/carbon nitride foam with hierarchical porosity for oil capture and chemical fixation of CO_2. Adv. Funct. Mater. https://doi.org/10.1002/adfm.201700706.

59. Bi, H., Xie, X., Yin, K., Zhou, Y., Wan, S., He, L., Xu, F., Banhart, F., Sun, L., and Ruoff, R.S. (2012). Spongy graphene as a highly efficient and recyclable sorbent for oils and organic solvents. Adv. Funct. Mater. *22*, 4421–4425.

60. Du, R., Cao, X., Feng, Q., Zhao, Q., Li, P., Deng, S., Shi, L., and Zhang, J. (2016). Microscopic dimensions engineering: stepwise manipulation of the surface wettability on 3D substrates for oil/water separation. Adv. Mater. *28*, 936–942.

61. Hayase, G., Kanamori, K., Fukuchi, M., Kaji, H., and Nakanishi, K. (2013). Facile synthesis of marshmallow-like macroporous gels usable under harsh conditions for the separation of oil and water. Angew. Chem. Int. Ed. *52*, 1986–1989.

62. Liang, H.-W., Guan, Q.-F., Chen, L.-F., Zhu, Z., Zhang, W.-J., and Yu, S.-H. (2012). Macroscopic-scale template synthesis of robust carbonaceous nanofiber hydrogels and aerogels and their applications. Angew. Chem. Int. Ed. *51*, 5101–5105.

63. Zhang, Y., Wei, S., Liu, F., Du, Y., Liu, S., Ji, Y., Yokoi, T., Tatsumi, T., and Xiao, F.-S. (2009). Superhydrophobic nanoporous polymers as efficient adsorbents for organic compounds. Nano Today *4*, 135–142.

64. Li, A., Sun, H.-X., Tan, D.-Z., Fan, W.-J., Wen, S.-H., Qing, X.-J., Li, G.-X., Li, S.-Y., and Deng, W.-Q. (2011). Superhydrophobic conjugated microporous polymers for separation and adsorption. Energy Environ. Sci. *4*, 2062–2065.

65. Jiang, Z.-R., Ge, J., Zhou, Y.-X., Wang, Z.U., Chen, D., Yu, S.-H., and Jiang, H. (2016). Coating sponge with a hydrophobic porous coordination polymer containing a low-energy CF_3-decorated surface for continuously

pumping recovery of an oil spill from water. NPG Asia Mater. *8*, e253.

66. Aussillous, P., and Quéré, D. (2001). Liquid marbles. Nature *411*, 924–927.

67. Gao, W., Lee, H.K., Hobley, J., Liu, T., Phang, I.Y., and Ling, X.Y. (2015). Graphene liquid marbles as photothermal miniature reactors for reaction kinetics modulation. Angew. Chem. Int. Ed. *54*, 3993–3996.

68. Dupin, D., Armes, S.P., and Fujii, S. (2009). Stimulus-responsive liquid marbles. J. Am. Chem. Soc. *131*, 5386–5387.

69. Xue, Y., Wang, H., Zhao, Y., Dai, L., Feng, L., Wang, X., and Lin, T. (2010). Magnetic liquid marbles: a "precise" miniature reactor. Adv. Mater. *22*, 4814–4818.

70. Wang, D., Zhu, L., Chen, J.-F., and Dai, L. (2016). Liquid marbles based on magnetic upconversion nanoparticles as magnetically and optically responsive miniature reactors for photocatalysis and photodynamic therapy. Angew. Chem. Int. Ed. *55*, 10795–10799.